Computational Vibrational Spectroscopy of Hydrophilic Drug Irinotecan

Bojana Koteska, Anastas Mishev
Faculty of Computer Science and Engineering
Skopje, Macedonia
email:bojana.koteska@finki.ukim.mk
email:anastas.mishev@finki.ukim.mk

Ljupco Pejov
Institute of Chemistry
Faculty of Natural Sciences and Mathematics
Skopje, Macedonia
email:ljupcop@pmf.ukim.mk

Maja Simonoska Crcarevska, Jasmina Tonic Ribarska,
Marija Glavas Dodov
Institute of Pharmaceutical Technology, Center of Pharmaceutical Nanotechnology
Faculty of Pharmacy
Skopje, Macedonia
email:msimonoska@ff.ukim.edu.mk
email:jato@ff.ukim.edu.mk
email:magl@ff.ukim.edu.mk

***Abstract*—A computational study of structural and vibrational spectroscopic properties of hydrophilic drug irinotecane was carried out. Both static and dynamical approaches to the problem have been implemented. In the static ones, vibrational spectra of the title system were computed within the double harmonic approximation, diagonalizing the mass-weighted Hessian matrices. These were calculated for the minima on AM1, PM3, PM6 and B3LYP/6-31G(*d,p*) potential energy surfaces. Within the dynamical approach, atom-centered density matrix propagation scheme was implemented at AM1 level of theory. From the computed molecular dynamics trajectories at series of temperatures (ranging from 10 to 300 K), velocity-velocity autocorrelation function was calculated and the vibrational density of states was sequentially obtained by Fourier transformation. Comparison with the experimental data revealed that the employed density functional level of theory exhibited remarkable performances. Of all semiempirical theoretical levels, PM6 was found to perform best, comparable to B3LYP/6-31G(*d,p*) when lower-frequency region is in question.**

Keywords-theoretical vibrational spectroscopy; high-performance computing; computational modelling; drugs; density functional theory.

I. INTRODUCTION

The classical paradigm in pharmaceutical sciences concerning drug delivery systems has changed significantly upon the advent of nanoscience and nanotechnology [1]. This emerging research area has opened quite new possibilities in achieving appropriate administration and targeting of pharmacologically active substances. Appropriate drug delivery is of essential importance in medical treatment of diseases, as it can affect most important aspects of drugs' pharmacological activity, such as its pharmacokinetics, distribution, metabolism, as well as the direct therapeutic effect itself.

The field of drug delivery along with the efforts directed towards controlled release have exhibited a significant evolution in the last few decades: starting from matrix-incorporated, hydrogel-encapsulated and finally nanoparticle-encaged drug paradigm. In the context of previous discussion, finding the most appropriate system for drug administration and targeted delivery is of essential importance in current research in pharmaceutical sciences [1].

In the last period, it has been shown that complex delivery systems built up when a hydrophilic drug is entrapped into a nanoparticle composed of hydrophobic polymer exhibit remarkably controllable properties.

Recently [2], the hydrophilic drug irinotecane (in the form of hydrochloride) has been incorporated into nanoparticles built up by poly lactic-co-glycolic acid copolymer (PLGA) and co-adsorbed PEO-PPO-PEO (polyethylene oxide – polypropylene – polyethylene oxide) copolymer. The formulations were designed by a planned experiment approach, and the nanoparticle-drug interaction upon encapsulation was studied by differential scanning calorimetry (DSC) and Fourier transform infrared (FTIR) spectroscopy. Subtle changes in the IR spectral properties of predominantly the co-polymer part of this complex system were used to derive conclusions about the drug incorporation into the nanoparticles and the nature of nanoparticle-drug interactions. Due to the inherent complexity and size of this multi-component system, to get an in-depth understanding of the mentioned phenomena, it is of essential importance to carry out theoretical simulations along with the spectroscopic experiments. In the course of the main aim to understand the vibrational spectroscopic, as well as energetic aspects of the nanoparticle-drug interactions, in the present study we carry

Copyright (c) IARIA, 2016. ISBN: 978-1-61208-501-2

out a computational study of vibrational dynamics of the hydrophilic drug irinotecane. We rely on the contemporary theoretical approaches to the mentioned issue, which are yet computationally feasible for studies of the drug molecule itself, as well as the drug incorporated into the nanoparticle cage.

In Section 2, we describe the two computational methodologies – static and dynamic. Section 3 presents the results from the implementation of both computational methods and a short discussion. In Section 4, we provide the conclusion.

II. COMPUTATIONAL DETAILS

To be able to get an insight into the changes of geometry and vibrational force field of the irinotecan molecule upon its inclusion in the PLGA/PEO-PPO-PEO nanoparticles, one has to explore in details the corresponding aspects in the case of free molecular system. For that purpose, we have adopted the following computational methodology. Two computational approaches were actually implemented in our current study: static and dynamic one.

Within the static approach, the geometry of neutral irinotecan molecule was first optimized using Schlegel's gradient optimization algorithm [3]. This was done at density functional level of theory (DFT), as well as using semiempirical AM1 [4], PM3 [5] and PM6 [6] Hamiltonians.

DFT calculations were performed employing a combination of Becke's three-parameter adiabatic connection exchange functional (B3 [7]) with the Lee-Yang-Parr correlation functional (LYP [8]); this computational approach is denoted by the (B3-LYP) acronym in the computational chemistry literature. The Pople-style basis set 6-31G(*d*,*p*) was used for orbital expansion in solving the Kohn-Sham equations, which was done in an iterative manner. This basis set is flexible enough to account for necessary structural specificity of the studied molecule; it contains a set of *d*-type polarization functions on "heavy" (*i.e.*, non-hydrogen) atoms and set of *p*-type polarization functions on all hydrogen atoms. It has been already demonstrated in numerous studies that DFT results exhibit a remarkably good convergence with the basis set size and double-zeta quality basis sets (as the one implemented in the current study) are often quite sufficient for a wide variety of purposes. For numerical integration in the course of DFT calculations, we have used the pruned (75,302) grid, consisting of 75 radial shells and 302 angular points per shell (leading to approximately 7000 points per atom). Subsequently to location of the stationary points on the molecular potential energy hypersurfaces (PESs), we have performed vibrational frequency calculations for the corresponding geometries. These computations were carried out within the harmonic approximation (diagonalizing the mass-weighted Hessian matrix). The aim of harmonic vibrational analysis was two-fold: to examine the character of the located stationary point on the corresponding PES, as well as to compute the intramolecular vibrational frequencies. The absence of imaginary frequencies (*i.e.*, negative eigenvalues of the Hessian matrices) served as an indication that a true (real) minimum has been located on the corresponding PES (instead of a saddle-point, *i.e.*, transition structure).

Within the dynamical approach, we have used the atom-centered density-matrix propagation scheme (ADMP) quantum molecular dynamics methodology [9]. A series of ADMP simulations were carried out for the irinotecan molecule, under constant temperature conditions, employing semiempirical AM1 method. The temperature was kept constant by velocity scaling at each step of the dynamical simulation. Dynamical simulations of the studied system were carried out at 10, 100, 200 and 300 K. Dynamical vibrational spectral characteristics of the title system were computed from the results of dynamical simulations as explained further in the paper. Each dynamical simulation consisted of 2000 steps, and the initial kinetic energy was set to 51297 microHartrees. The fictitious electronic mass was set to 0.1 amu; simulation step size was set at 0.2 fs.

All quantum mechanical calculations in the present study were carried out with the Gaussian09 series of codes [10].

III. RESULTS AND DISCUSSION

In this Section, we provide the results from the static and dynamic approaches for finding the vibrational spectroscopy of hydrophilic drug irinotecan.

A. *Static approach*

The optimized geometry of irinotecan molecule at the B3LYP/6-31G(*d*,*p*) level of theory (*i.e.*, the minimum on the corresponding PES) is shown in Fig. 1.

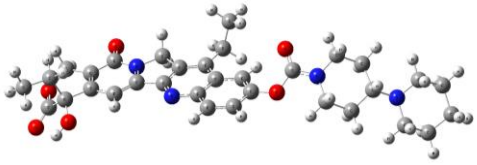

Figure 1. Optimized geometry of irinotecan at B3LYP/6-31G(*d*,*p*) level of theory.

As can be seen from Fig. 1, the structure of neutral free irinotecan is characterized by an intramolecular O-H…O hydrogen bond. The H…O distance in this intramolecular contact is 2.0054 Å.

Semiempirical levels of theory give quite similar structures for free irinotecan molecule, the main predicted structural differences being in the conformationally flexible intramolecular degrees of freedom. The structures corresponding to real minima on the AM1, PM3 and PM6 PESs of free irinotecane molecule are shown in Fig. 2. Perhaps the most notable difference in the predicted minimum-energy structures at the implemented semiempirical levels of theory is the conformational flexibility of the OH group. As can be seen from Fig. 2, both AM1 and PM3 levels of theory predict minimum energy structures in which the proton from the OH group is far below the plane in which the C-C=O fragment (containing the carbonyl group oxygen atom) lies. Such arrangement does not conform to an arrangement of atoms characteristic

Copyright (c) IARIA, 2016. ISBN: 978-1-61208-501-2

for a hydrogen bond. Obviously, therefore, these two semiempirical levels of theory fail to predict the existence of intramolecular hydrogen bond of the O-H…O type.

Contrary to AM1 and PM3 levels, however, the results obtained with the PM6 semiempirical Hamiltonian are similar with this respect to the DFT results. We are therefore apt to conclude that the PM6 semiempirical level of theory should be regarded as more reliable that AM1 and PM3 when structural consequences of specific intramolecular interactions are in question. Concerning the conformational flexibility of the mostly-aliphatic part of the molecule (with sp^3 hybridized carbon atoms), on the other hand, all levels of theory predict different conformational landscape generated by rotations around the C-O and O-N bonds. However, due to the absence of specific intramolecular interactions in this part of the molecule, such flexibility is in fact expected. Moreover, in presence of relatively low barriers to intramolecular torsional motions (*i.e.*, hindered rotations) of the mentioned types, the actual molecular structure may be an average of the thermally-induced dynamically interchanging configurations.

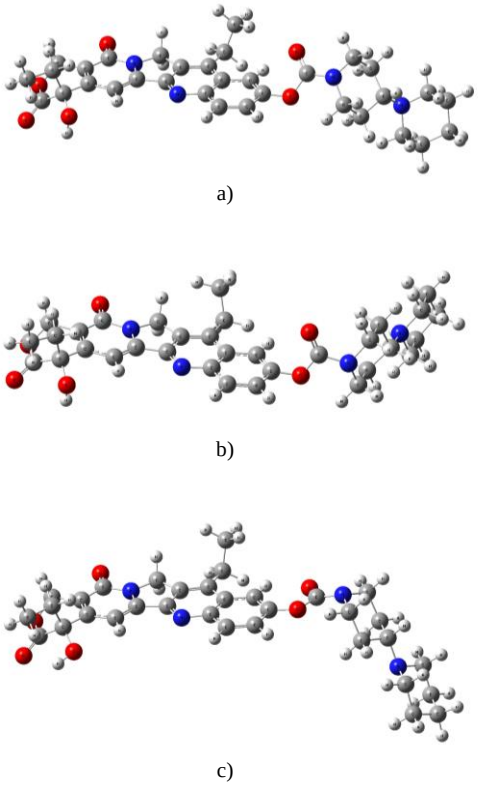

a)

b)

c)

Figure 2. Optimized geometry of irinotecan at semiempirical AM1 (a), PM3 (b) and PM6 (c) levels of theory.

The main aim of the present study is to establish a reliable computational methodology for prediction of vibrational spectroscopic properties of free irinotecan molecule, which could later be used for prediction of spectral changes as a consequence of inclusion of this molecule within PLGA/PEO-PPO-PEO nanoparticles, followed by subsequent adsorption on the inner, hydrophilic wall thereof.

We have therefore further computed the IR spectra of the title molecule at the employed theoretical levels, by diagonalization of mass-weighted Hessian matrix. Since this procedure essentially gives the harmonic vibrational frequencies, to account for the known systematic differences between experimental (anharmonic) values and the theoretical ones, as well as to account for the known systematic errors due to inherent assumptions to each of the employed theoretical models, we have scaled the initially computed vibrational wavenumbers with the established scaling factors [11]. The resulting IR spectra obtained by convoluting the delta-function spectra with Lorentzian functions with a half-width of 4 cm^{-1} are presented in Fig. 3.

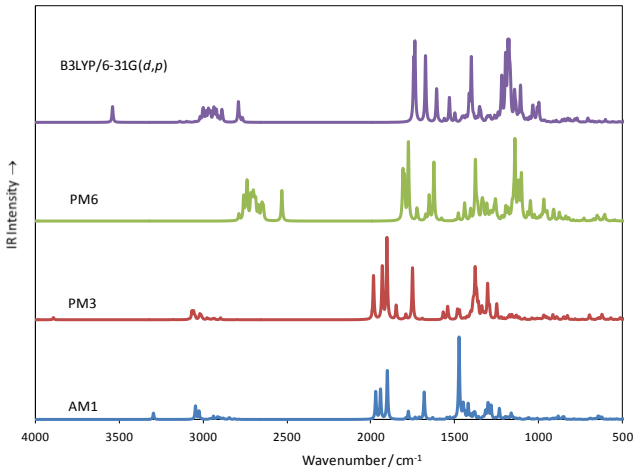

Figure 3. Theoretical IR spectra of free irinotecan in the MIR region computed at semiempirical AM1, PM3 and PM6, as well as at DFT B3LYP/6-31G(*d*,*p*) levels of theory.

As can be seen, the methods exhibit rather different performances when vibrational modes appearing above and around 3000 cm^{-1} are in question. However, as the experimental spectroscopic data have usually been collected in the region below 2500 (or 2000) cm^{-1}, this is the region that may be considered to be of primary importance in the context of present and also of upcoming studies of this molecular system, either isolated (gas-phase) or embedded within a condensed phase environment. When one considers the mentioned region, however, it becomes obvious even from visual inspection of the theoretical spectra that PM6 semiempirical approach performs rather comparably to the B3LYP/6-31G(*d*,*p*) "model chemistry", and thus is the method of choice for further studies of vibrational spectroscopic properties of irinotecan incorporated in PLGA/PEO-PPO-PEO nanoparticles. Such nanoparticles are rather large from computational viewpoint, with rather disordered structure viewed at molecular level. It is therefore of substantial interest to compare the performances of various computational methods with this respect. If the performances of a method with lower computational cost are comparable to those of a well-established computational approach (such as, e.g., B3LYP/6-31G(*d*,*p*)), it could be of high significance for prediction of changes of the vibrational spectroscopic signature of irinotecan molecule upon its

Copyright (c) IARIA, 2016. ISBN: 978-1-61208-501-2

incorporation (encapsulation)/inner wall adsorption within the mentioned nanoparticles serving as drug-carriers. Finally, we compare the experimental ATR FTIR spectra of irinotecan hydrochloride with the B3LYP/6-31G(*d*,*p*) theoretical one in Fig. 4.

As can be seen, the agreement between theory and experiment is remarkable.

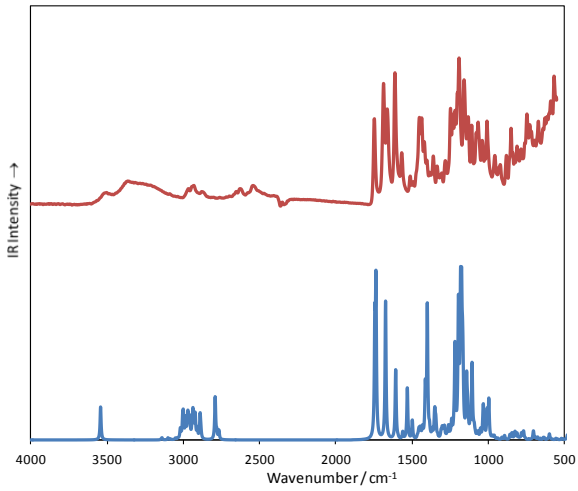

Figure 4. Theoretical IR spectrum of free irinotecan computed at DFT B3LYP/6-31G(*d*,*p*) level of theory (lower curve), together with the experimental ATR FTIR spectrum of irinotecan hydrochloride.

While the spectral region above and around 3000 cm^{-1} is dominated by bands due to OH and CH stretching vibrations, the lower frequency region (usually below 2000 cm^{-1}) is a bit more complex and contains the so-called molecular fingerprint region. This spectral region is dominated by bands due to carbonyl (C=O) stretching vibrations in two spatially distant segments of irinotecan molecule, appearing at about 1744, 1737 and 1674 cm^{-1} in the B3LYP/6-31G(*d*,*p*) theoretical spectrum (IR intensities are 349, 503 and 469 km mol^{-1} respectively). The carbonyl stretching band appearing at lowest frequencies is due to the carbonyl group attached to the heterocyclic aromatic ring. Therefore, partial delocalization of electronic density into the aromatic ring leads to lowering of the corresponding C=O bond force constant value and consequently lower C=O stretching vibration as compared to the other intramolecular carbonyl moieties which are not attached to aromatic systems. Note that the band appearing at about 1608 cm^{-1} (with IR intensity of about 204 km mol^{-1}) is due to a mode containing a significant contribution of the C=O stretching coordinate (along with the C=C stretching ones and in-plane CCH bending one – δ(CCH)). Yet another band due to the aromatic C=C stretching mode appearing at about 1532 cm^{-1} is of appreciable IR intensity (~175 km mol^{-1}). The lower-frequency part of the spectrum is dominated by intensive bands due to CH and CH_2 bending, scissoring and wagging modes appearing at 1414 and 1401 cm^{-1} (IR intensities being 151 and 447 km mol^{-1} respectively) and further at about 1220, 1198, 1180, 1170, 1143 and as low as about 1000 cm^{-1} (with IR intensities varying from 100 to about 400 km mol^{-1}).

B. *Dynamical approach*

In a realistic system relevant to the present study, the molecules are not static, and the processes take place at temperatures high above absolute zero. The static quantum chemical approximation is therefore insufficient to account for all dynamical features related to drug incorporation and adsorption on the inner walls of nanoparticles. In the present pilot study, we employ the atom centered density matrix propagation approach (ADMP) to study the dynamical aspects of the tackled problem. In comparison to other studies related to theoretical vibrational spectroscopy of drug molecules, one of the main aims of the present study is to make a thorough comparison of the performances of variety of static methodologies (based on exploration of molecular PES and subsequent computation of the second derivative matrix) with the dynamical ones, such as the presently implemented ADMP one. From a fundamental viewpoint, ADMP methodology is an extended Lagrangian approach to molecular dynamics, based on usage of Gaussian basis functions, in which it is the density matrix that is being propagated [9]. The system's extended Lagrangian is written in the form:

$$L = \frac{1}{2}Tr\left(V^T M V\right) + \frac{1}{2}\mu Tr(WW) - E(R,P) - Tr[\Lambda(PP-P)] \quad (1)$$

In (1), *M*, *R* and *V* represent the nuclear masses, positions and velocities; *P*, *W* and μ denote the density matrix, density matrix velocity and the fictitious mass for the electronic degrees of freedom, correspondingly. Λ, on the other hand, is a Lagrangian multiplier matrix, used to impose the constraints on the total number of electrons in the system and on the idempotency of the density matrix. The Euler-Lagrange equations for density matrix propagation may subsequently be obtained applying the principle of stationary action. These equations can be written in the form:

$$\mu\frac{d^2P}{dt^2} = -\left[\left.\frac{\partial E(R,P)}{\partial P}\right|_R + \Lambda P + P\Lambda - \Lambda\right] \quad (2)$$

$$M\frac{d^2R}{dt^2} = -\left.\frac{\partial E(R,P)}{\partial R}\right|_P \quad (3)$$

Equations (2) and (3) were integrated in the present study by the velocity Verlet algorithm, under the conditions described technically in the Computational details section. Since we deal with a finite-size molecular system, periodic boundary conditions have not been imposed in the present study.

From the computed ADMP molecular dynamics trajectory, we have subsequently computed the velocity-velocity autocorrelation function, defined as [12]:

Copyright (c) IARIA, 2016. ISBN: 978-1-61208-501-2

$$C(t) = \frac{\langle \vec{v}(0) \cdot \vec{v}(t) \rangle}{\langle \vec{v}(0) \cdot \vec{v}(0) \rangle} \quad (4)$$

From the last quantity, the vibrational density of states power spectrum $\Phi(\omega)$ may be computed as a squared $F(\omega)$, where $F(\omega)$ is Fourier transform of $C(t)$:

$$F(\omega) = \frac{1}{\sqrt{2\pi}} \int_{-\infty}^{+\infty} C(t) \cdot \exp(i\omega t) dt \quad (5)$$

In the presently studied case, we have computed $F(\omega)$ by fast Fourier transformation technique (FFT), using Welch window function of the form:

$$w(n) = 1 - \left(\frac{n - \frac{1}{2}(N-1)}{\frac{1}{2}(N+1)} \right)^2 \quad (6)$$

where N denotes the total number of data points, and n is the n-th data point. Computations of Fourier transformation using the mentioned window function were carried out with the OriginPro 2016 program [13].

Throughout the quantum molecular dynamics simulation the total angular momentum of the system was conserved to an exceptionally high degree (< 10^{-11} $\hbar$) – Fig. 5, as a consequence of the usage of projection methods to remove the residual angular forces.

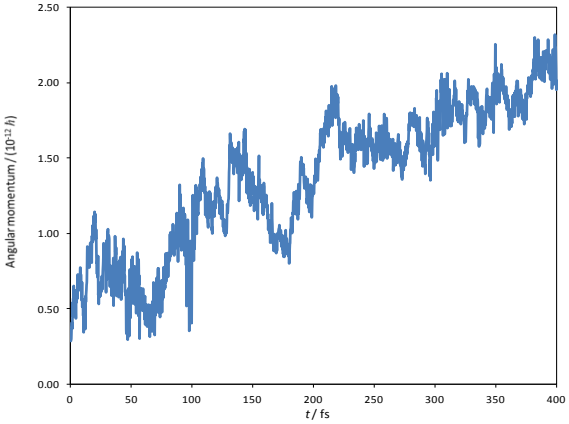

Figure 5. The total angular momentum of the studied system as a function of simulation time.

The RMS idempotency was conserved to better than 10^{-12} throughout all the simulation steps at all simulation temperatures. Fig. 6, Fig. 7 and Fig. 8 depict the time evolution of electronic kinetic energy (*i.e.*, density matrix kinetic energy), nuclear kinetic energy, as well as total energy in case of ADMP simulation of free irinotecane at temperature of 100 K.

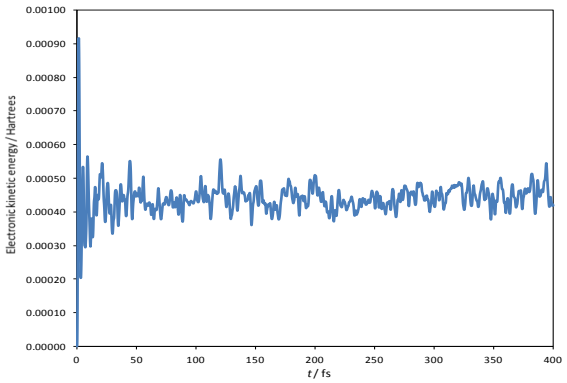

Figure 6. Time evolution of the electronic kinetic energy (density matrix kinetic energy).

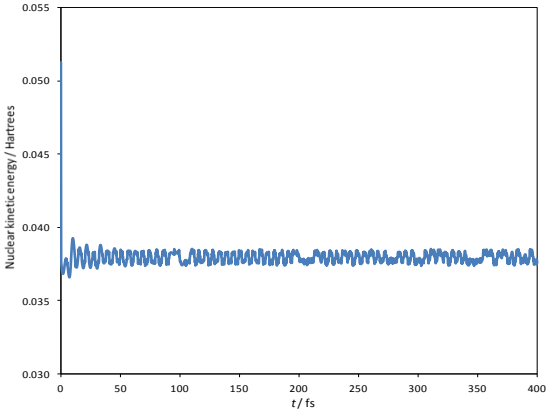

Figure 7. Time evolution of the nuclear kinetic energy.

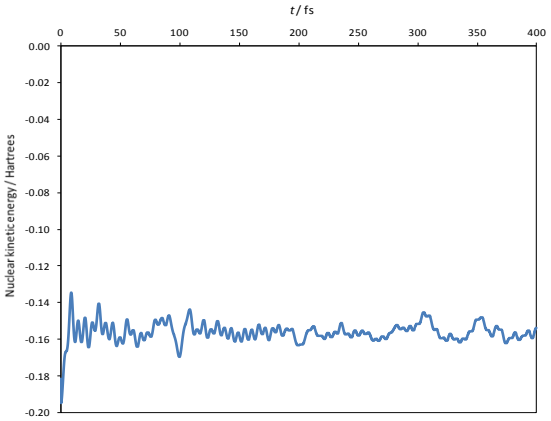

Figure 8. Time evolution of the total energy.

Fig. 9 and Fig. 10 depict the vibrational spectra of free irinotecane molecule computed by Fourier transformation of the velocity-velocity autocorrelation functions at 100 and 300 K.

As we are primarily interested in the appearance of the lower-frequency spectral region of the title molecular system, only the spectral range below 2000 cm^{-1} is presented in these figures.

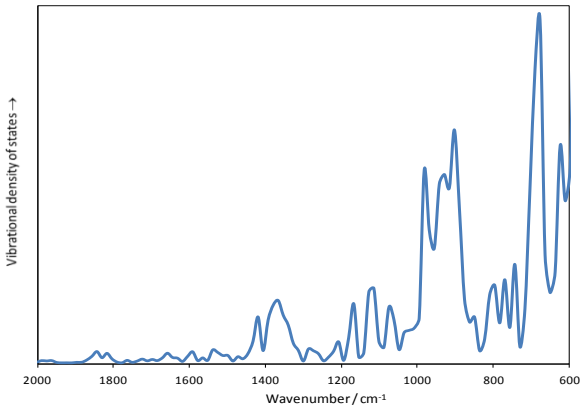

Figure 9. Vibrational spectrum of irinotecane computed from the ADMP simulation at 300 K.

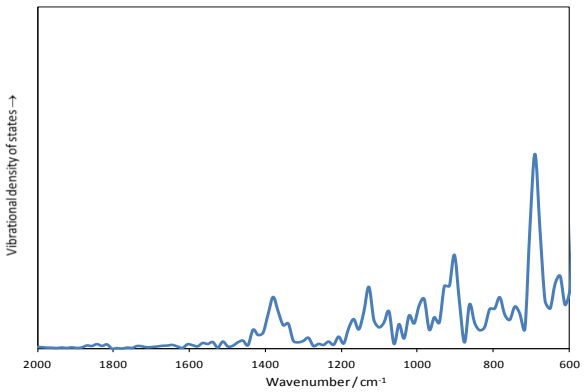

Figure 10. Vibrational spectrum of irinotecane computed from the ADMP simulation at 100 K.

IV. CONCLUSIONS AND DIRECTIONS FOR FURTHER WORK

In the present study, we have carried out a theoretical vibrational spectroscopic study of hydrophilic drug irinotecane. Semiempirical AM1, PM3 and PM6 levels of theory were applied, along with the B3LYP/6-31G(*d*,*p*) DFT level. The DFT level was found to reproduce remarkably well the experimental FTIR spectra of the title system. Of all semiempirical levels the PM6 approach was found to perform comparable to B3LYP. Vibrational spectra were also computed from ADMP molecular dynamics simulations at series of temperatures. The conclusions derived have established an appropriate choice of computational methodologies for upcoming studies of irinotecan molecule entrapped in PLGA/PEO-PPO-PEO nanoparticles. The approach elaborated in this paper has two main advantages. The first one concerns the computational cost of the prediction of IR spectral features of drug molecules (such as the presently studied one), which is significantly reduced by using appropriate semiempirical Hamiltonian, while the results remain of DFT-like (B3LYP) quality. The second advantage is the explicit account of dynamical features in computation of the vibrational spectra of the title system by using ADMP methodology.

ACKNOWLEDGMENT

This work was supported in part by the European Union's Horizon 2020 research and innovation programme, project Virtual Research Environment for Regional Interdisciplinary Collaboration in Southeast Europe and Eastern Mediterranean VI-SEEM [675121].

REFERENCES

[1] M. W. Tibbitt, J. E. Dahlman, and R. Langer, "Emerging Frontiers in Drug Delivery", Journal of the American Chemical Society, vol. 138, 2016, pp. 704-717, doi: 10.1021/jacs.5b09974.

[2] M. Simonoska Crcarevska et al., "Definition of formulation design space, in vitro bioactivity and in vivo biodistribution for hydrophilic drug loaded PLGA/PEO–PPO–PEO nanoparticles using OFAT experiments", European Journal of Pharmaceutical Sciences, vol. 49, 2013, pp. 65-80, doi:10.1016/j.ejps.2013.02.004.

[3] H. B. Schlegel, "Optimization of equilibrium geometries and transition structures", Journal of Computational Chemistry, vol. 3, 1982, pp. 214-218, doi: 10.1002/jcc.540030212.

[4] M. J. S. Dewar and W. Thiel, "Ground states of molecules. 38. The MNDO method. Approximations and parameters", Journal of the American Chemical Society, vol. 99, 1977, pp. 4899-4907, doi: 10.1021/ja00457a004.

[5] J. J. P. Stewart, "Optimization of parameters for semiempirical methods I. Method", Journal of Computational Chemistry, vol. 10, 1989, pp. 209-220, doi: 10.1002/jcc.540100208.

[6] J. J. P. Stewart, "Optimization of parameters for semiempirical methods V: modification of NDDO approximations and application to 70 elements", Journal of Molecular Modeling, vol. 13, 2007, pp. 1173-1213, doi: 10.1007/s00894-007-0233-4.

[7] A. D. Becke, "Density-functional exchange-energy approximation with correct asymptotic behavior", Physical Review A, vol. 38, 1988, pp. 3098-3100, doi:http://dx.doi.org/10.1103/PhysRevA.38.3098.

[8] C. Lee, W. Yang, and R. G. Parr, "Development of the Colle-Salvetti correlation-energy formula into a functional of the electron density", Physical Review B, vol. 37, 1988, pp. 785-789, doi: 10.1103/PhysRevB.37.785.

[9] S. S. Iyengar et al., "Ab initio molecular dynamics: Propagating the density matrix with Gaussian orbitals. II. Generalizations based on mass-weighting, idempotency, energy conservation and choice of initial conditions", Journal of Chemical Physics, vol. 115, 2001, pp. 10291-10302, doi: 10.1063/1.1416876.

[10] M. J. Frisch et al., Gaussian 09, Revision A.1, Gaussian, Inc., Wallingford CT, 2009.

[11] National Institute of Standards and Technology, Precomputed Vibrational Scaling Factors, http://cccbdb.nist.gov/vibscalejust.asp (accessed 15.04.2016).

[12] D. A. McQuarrie, Statistical Mechanics, Harper&Row, New York, 1976.

[13] OriginPro 2016, 1991-2015 OriginLab Corporation. [Online]. Available from: http://www.originlab.com/2016 .

Copyright (c) IARIA, 2016. ISBN: 978-1-61208-501-2